Compact Car-Body Surface Design with T-spline Surface

Xue Xiang(薛翔), *Zhou Laishui*(周来水)*

College of Mechanical and Electrical Engineering, Nanjing University of Aeronautics and Astronautics, Nanjing, 210016, P. R. China

(Received 24 April 2014; revised 11 August 2014; accepted 3 September 2014)

Abstract: Creating proper B-spline surface models is a very challenging task for designers in car-body surface design. Due to the tensor-product structure of B-spline surface, some undesirable issues of the redundant control points addition, incomplete surface definition and the difficulty of trimming boundary alteration frequently occur, when designing the car-body surface with B-spline surfaces in local-feature-lines construction, full-boundary-merging and visual surface trimming. A more efficient approach is proposed to design the car-body surface by replacing B-spline surface with classical T-spline surface. With the local refinability and multilateral definition offered by T-spline surface, those designing issues related with B-spline surface can be overcomed. Finally, modeling examples of the door, hood and rear-window are given to demonstrate the advantage of T-spline surface over B-spline surface in car-body surface design.

Key words: car-body surface design; T-spline surface; local-feature-line construction; surface merging; surface trimming

CLC number: TP391.7 **Document code**: A **Article ID**: 1005-1120(2014)06-0615-07

1 Introduction

Car-body surface design is a very complex and challenging procedure[1], which needs the designer to perfectly blend the flexible and rigid design elements together. For instance, to achieve a stylish shape in aesthetics and to meet the aerodynamic demand in engineering, the local-feature-line often requires to be built upon car-body surface. For a complex and cumbersome car-body model, adjacent car-body surfaces sometimes need to be merged for getting a compact surface model that is easily edited. Besides, in addition to the quadrilateral surface frequently used in car-body design, the multilateral surface also needs to be built via the surface trimming in many cases. Since B-spline surfaces have the favorable local controllability and can be piecewisely defined with ease[2], they are often selected for designing car-body surfaces.

When using B-spline surface to design car-body surfaces, some undesirable problems occur because of the tensor-product scheme of B-spline surface, especially during the local-feature-line construction, adjacent incompatible surfaces merging, and the visual trimming of surface. When building the local-feature-line over car-body surface, for instance, new control points are always added in groups across the entire B-spline surface via knot-insertion, but many of them are redundant control points that are useless for the construction of local-feature-line. For merging two adjacent car-body surfaces with incompatible boundaries, the knot-insertion is also often applied to obtain compatible boundary conditions before the surface merging. However, the merged car-body surface still has the problem of redundant control points, because new control points are also added onto B-spline surface in groups through the knot-insertion. Besides, after applying the visual trimming to build multilateral surface upon car-body, initial B-spline surface definition and the control polygon of car-body surface remains unchanged and no extra control points are added around the trimming boundary. Therefore, the visually-trimmed car-body surface

* **Corresponding author**: Zhou Laishui, Professor, E-mail: zlsme@nuaa.edu.cn.

not only does not have a complete surface definition, but also the trimming boundary is inconvenient to be edited. Many researchers improve the tensor-product B-spline surface, such as the hierarchical B-spline surface[3,4], the locally-refined B-spline surface[5,6], and the B-spline wavelet surface[7,8]. However, these variants of B-spline surfaces still do not resolve those previously mentioned problems occurred during the car-body surface design based on B-spline surface.

Sederberg, et al. developed the classical T-spline surface in 2003[9], and improved its local refinement algorithm in 2004[10]. Unlike B-spline surface, T-spline surface totally frees itself from the restriction of traditional tensor-product surface, thus it has flexible local surface refinement and multilateral surface definition. Except classical T-spline surface, Tong, et al. introduced the implicit T-spline surface[11], Deng, et al. developed the polynomial splines over hierarchical T-meshes (PHT-splines)[12], and Chen, et al. proposed the modified T-spline surface[13]. Although implicit T-spline surface is good at fitting unorganized points collection during surface reconstruction, it is far less convenient for interactive surface design than classical T-spline surface because of its implicit surface description. PHT-splines and modified T-spline surface are quite useful in fitting mesh models and surface simplification, but they are both defined over hierarchical T-meshes and need to maintain a much more complex hierarchical data structure than classical T-spline surface. Therefore, classical T-spline surface is more suitable for interactively designing the required surface than implicit T-spline surface, PHT-splines and modified T-spline surface.

In the paper we replace common B-spline surface with classical T-spline surface to improve the car-body surface design in local-feature-line construction, incompatible full-boundary-merging and surface trimming upon multilateral domain, respectively. Some undesirable problems related with B-spline surface can be solved by using classical T-spline surface, making the surface design upon car-body become more efficient and convenient. In following sections, T-spline surface refers to the classical T-spline surface.

2 T-spline Surface

Different from tensor-product B-spline surface, T-spline surface comes from the definition of point-based spline surface (PB-splines)[14,15], but it is built over a two-dimensional grid called T-mesh. Each T-mesh is formed by vertically and horizontally combining a set of unit-blocks together, and every B-spline function B_k of T-spline surface is locally defined at a control node upon T-mesh. Since every B_k relates to a control point P_k of T-spline surface, thus the T-mesh is topologically identical to the control polygon of T-spline surface, as seen in Fig. 1. Besides, T-mesh has two knot vectors of $\boldsymbol{U}=[u_0,u_1,\cdots,u_p]$ and $\boldsymbol{V}=[v_0,v_1,\cdots,v_q]$, which can be readily converted to two knot-spacing vectors of $\boldsymbol{D}=[d_0,d_1,\cdots,d_{p-1}]$ and $\boldsymbol{E}=[e_0,e_1,\cdots,e_{q-1}]$ via $d_k=u_{k+1}-u_k$ and $e_k=v_{k+1}-v_k$. Based on the PB-splines definition, T-spline surface is mathematically described by the $S_T(u,v)=\sum_{k=1}^{z}B_k(u,v)P_k$, in which $B_k(u,v)$ is the B-spline function locally defined over T-mesh and P_k is the control point of T-spline surface.

T-spline surface can be not only built over a quadrilateral T-mesh, but also it can be constructed upon a multilateral T-mesh, like the O-shaped multilateral T-mesh and T-spline surface shown in Fig. 1. The quadrilateral T-mesh can be denoted as one type of 2×2 T-mesh, because it always has two vertical and two horizonal boundaries. Similarly, the multilateral T-mesh can be denoted as another type of $m\times m$ T-mesh with $m>2$. For example, the O-shaped multilateral T-mesh in Fig. 2 is a 4×4 T-mesh by having four

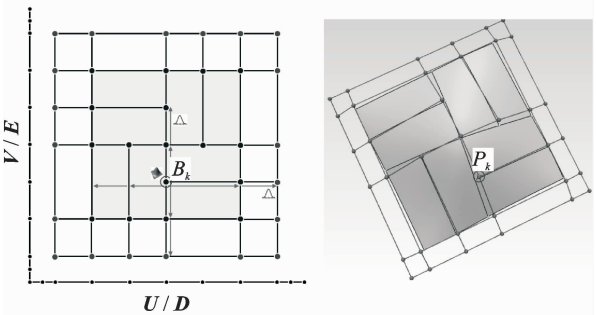

Fig. 1 T-mesh and T-spline surface

vertical and four horizonal boundaries. Except for the multilateral T-mesh and control polygon, multilateral T-spline surface is the same as the quadrilateral T-spline surface, such as the local refinability and surface definition.

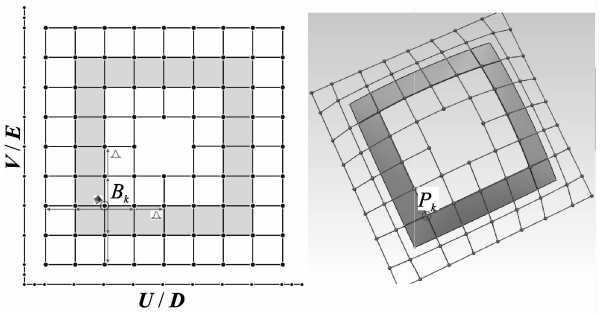

Fig. 2 Multilateral T-mesh and T-spline surface

3 Full-Row-Column T-spline Surface

Although B-spline surface and T-spline surface adopt distinct surface definitions, but any B-spline surface can be exactly converted into a full-row-column T-spline surface. This converting process is achieved by re-defining the B-spline function B_{ij} of B-spline surface over the uniform T-mesh of full-row-column T-spline surface as B_k, and establishing topology connections among B-spline functions defined over T-mesh. For instance in Fig. 3(a), B-spline functions are located on the control grid of B-spline surface before surface conversion, and they are defined by two knot vectors of $\boldsymbol{U}$ and $\boldsymbol{V}$. After surface conversion, B-spline functions are placed over the uniform T-mesh of full-row-column T-spline surface in Fig. 3(b), and they are defined through two knot vectors of $\boldsymbol{U}$ and $\boldsymbol{V}$, or two knot-spacing vectors of $\boldsymbol{D}$ and $\boldsymbol{E}$.

After converting B-spline surface into the full-row-column T-spline surface, the shape and control polygon of surface remain unchanged, but the surface construction is fundamentally changed. The surface equation is also converted from the $S_B(u,v) = \sum_{i=1}^{m}\sum_{j=1}^{n} B_{ij}(u,v)P_{ij}$ based on tensor-product surface, to the $S_T(u,v) = \sum_{k=1}^{z} B_k(u,v)P_k$ based upon PB-splines.

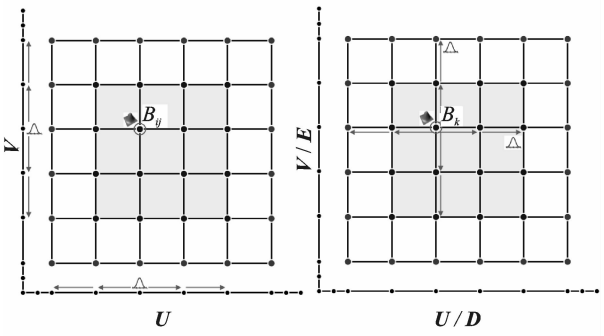

(a) Control grid of B-spline surface (b) Uniform T -mesh of full-row-column T-spline surface

Fig. 3 Re-definition of B-spline functions during surface conversion

Besides, the surface refining operation becomes more flexible after the conversion. In Fig. 4, control points have to be added in full rows or columns when refining the B-spline surface. In contrast, the converted full-row-column T-spline surface can be more flexibly refined by adding local rows and columns of control points, as shown in Fig. 5.

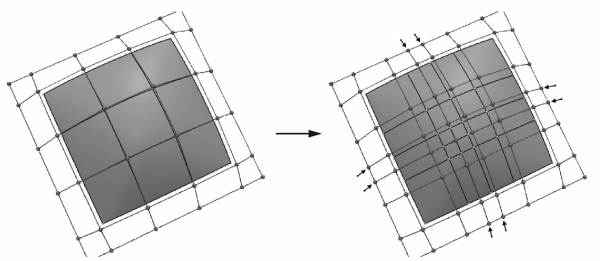

Fig. 4 B-spline surface refinements

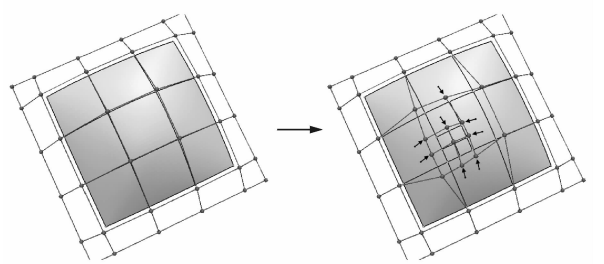

Fig. 5 Full-row-column T-spline surfaces refinements

4 Local-Feature-Line Construction upon T-spline Surface

When building the local-feature-line upon car-body surface through B-spline surface refine-

ment, many redundant control points are simultaneously produced after refining B-spline surface via the knot-insertion, and these control points are useless for the construction of local-feature-line. For instance in Fig. 6(a), the car door is initially described by a B-spline surface. If we apply B-spline surface refinements to build the local-feature-line shown in Fig. 6(c), four full rows and two full columns of control points need to be added as seen in Fig. 6(b), putting 62 control points onto the door surface.

If the B-spline surface in Fig. 6(a) is converted into the full-row-column T-spline surface in Fig. 7(a), the local-feature-line can be more efficiently built by merely adding four local rows and two local columns of control points, as seen in Fig. 7(b). Only 22 control points need to be added for creating the local-feature-line shown in Fig. 7(c), and they just account for 35% of the control points added in the context of B-spline surface in Fig. 6. Therefore, the resulting door surface built with the local-feature-line can be described by a more compacter T-spline surface with less control points than a B-spline surface with redundant control points, through a comparison between Fig. 6(b) and Fig. 7(b).

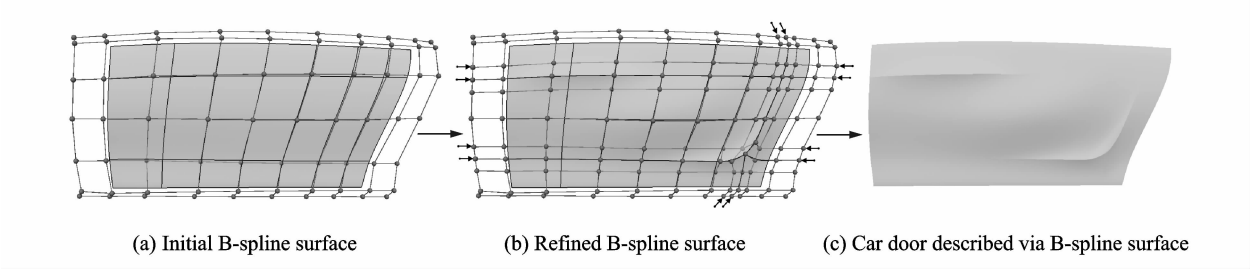

Fig. 6 Local-feature-line construction upon B-spline surface

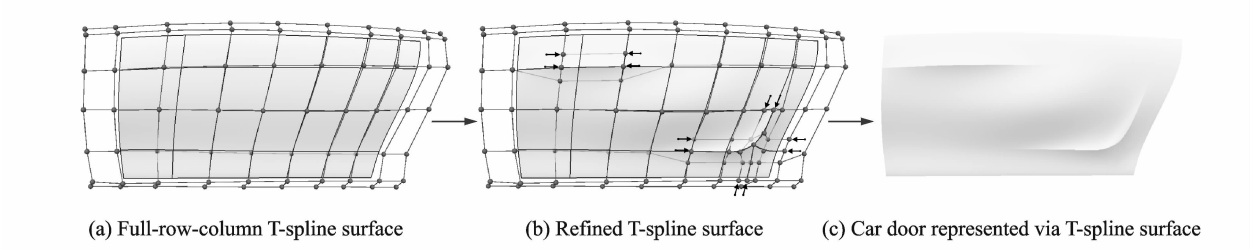

Fig. 7 Local-feature-line building over full-row-column T-spline surface

5 Adjacent Incompatible T-spline Surfaces Merging

Before merging two adjacent car-body surfaces with incompatible boundaries, the knot-insertion is also frequently used to make neighboring surfaces achieve compatible boundary conditions. Because of the addition of control points across the entire surface when refining incompatible B-spline surfaces via the knot-insertion for surface merging, the merged car-body surface still has the problem of redundant control points. In Fig. 8(a), the hood of car is composed of three B-spline surfaces, which do not have compatible boundary conditions to each other. In Fig. 8(b), these B-spline surfaces are refined to be compatible along their common boundaries by adding full-rows of control points, and then they are merged into a new B-spline surface representing the hood in Fig. 8(c). We need to add 54 control points throughout the surface merging based on B-spline surface refinements. If these three B-spline surfaces are converted into three full-row-column T-spline surface in Fig. 9(a), the more efficient T-spline surface refinement can be applied to make adjoining surfaces compatible along their shared boundaries. In Fig. 9(b), neighboring T-spline surface are refined to have compatible boundary

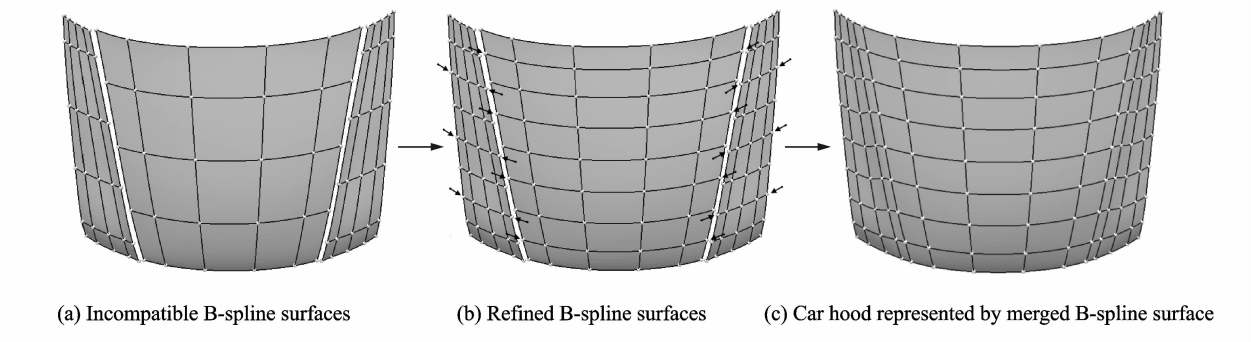

Fig. 8 Surface merging based on B-spline surface refinements

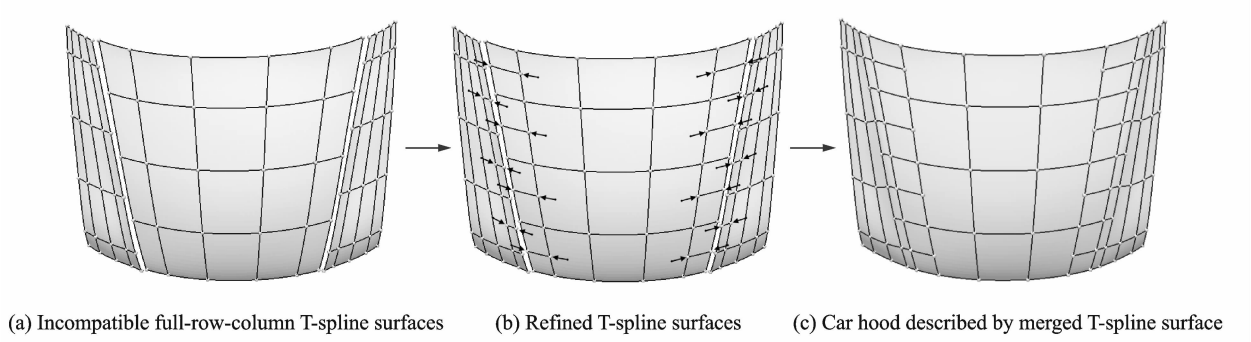

Fig. 9 Surface merging based on T-spline surface refinements

condicontions by adding local-rows of trol points, and they are merged into a new T-spline surface with less control points to describe the hood in Fig. 9(c). Just 28 control points need to be added this time, and they only account for 51% of the control points added in the case of B-spline surface merging in Fig. 8. By comparing Fig. 8(c) with Fig. 9(c), the merged hood surface has a more compacter T-spline surface description than a B-spline surface representation.

6 Geometrical Trimming of T-spline Surface

When creating a car-body surface upon multilateral domain through the visual trimming of B-spline surface, the trimming region is firstly specified with a trimming curve or loop, and is visually hidden during the surface rendering, yielding a visually-trimmed car-body surface. For example in Fig. 10(a), the rear-window of car is initially represented by a B-spline surface, and a trimming loop is used to specify the trimming region. By hiding the trimming region upon B-spline surface, the visually-trimmed rear-window surface is acquired in Fig. 10(c). However, the surface definition and control polygon of B-spline surface are not changed throughout the visual trimming in Fig. 10(b). Thus, the visually-trimmed rear-window surface lacks a complete surface definition and its trimming boundary is less convenient to be edited.

Once the B-spline surface is converted into a full-row-column T-spline surface, the converted surface can be geometrically trimmed into a multilateral T-spline surface, which has a complete surface definition and the trimming boundary is easy to be altered as well. In the following, we specifically describe the geometrical trimming of T-spline surface based on the surface trimming of rear-window.

Fig. 11(a) shows the rear-window represented through B-spline surface, upon which the trimming region is specified. In Fig. 11(b), this B-spline surface is refined via knot insertion, adding two full-rows and two full-columns of con-

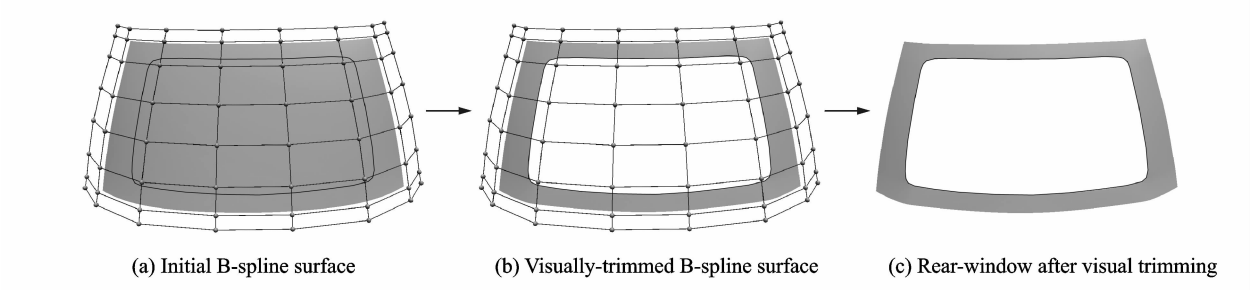

Fig. 10 Visual trimming of B-spline surface

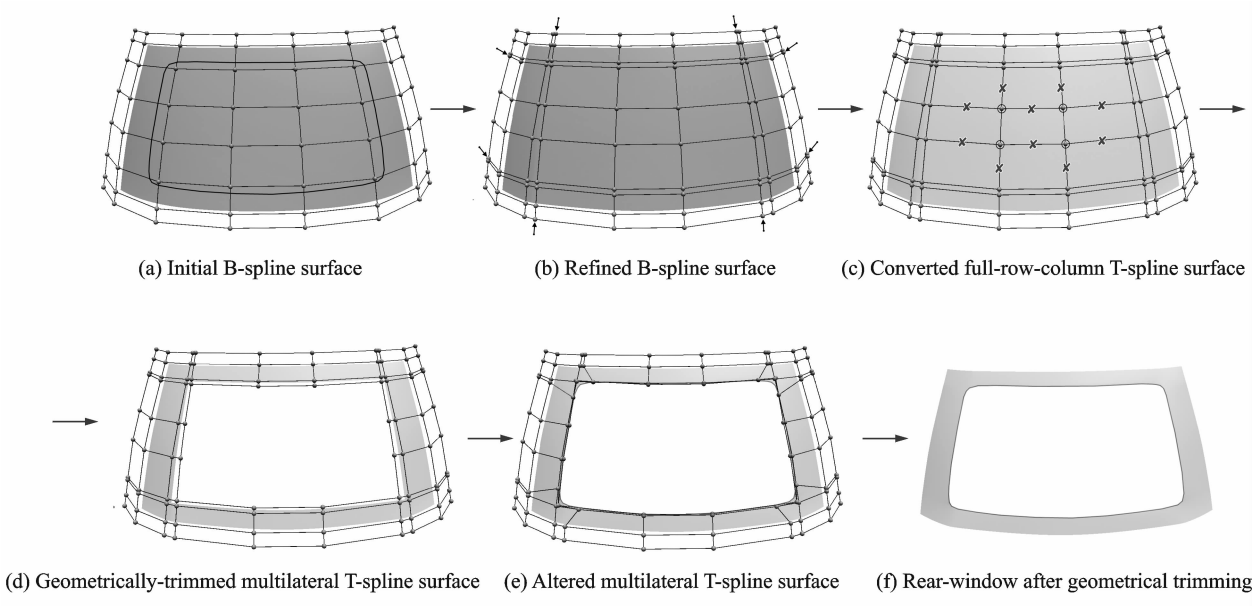

Fig. 11 Geometrical trimming of T-spline surface

trol points to isolate the trimming region. The refined B-spline surface is then converted into a full-row-column T-spline surface shown in Fig. 11(c). By removing four inner control points within the trimming region along with surrounding vertical and horizonal control lines, the converted full-row-column T-spline surface is geometrically trimmed into a multilateral T-spline surface in Fig. 11(d). After the geometrical trimming of T-spline surface, the trimming boundary can be readily modified by adjusting those newly-added control points, yielding the needed rear-window surface in Fig. 11(f).

Compared with the visual trimming of B-spline surface, the geometrical trimming of T-spline surface is slightly more complex because it includes four consecutive steps of the surface refinement, surface conversion, control points removement, and control points adjustment. However, the geometrically-trimmed car-body surface with not only has a complete surface definition, but also the trimming boundary is more readily altered.

7 Conclusions

To achieve the more efficient local-feature-line construction, full-boundary-merging along incompatible boundaries and the surface trimming upon multilateral domain, we adopt the more flexible T-spline surface rather than rigid B-spline surface to design the required car-body surface in the paper. As a result, the local-feature-line construction upon car-body surface and the incompatible full-boundary-merging between adjacent car-body surfaces can be accomplished more efficiently in T-spline surface by adding local control

points. Additionally, the geometrically trimmed car-body surface not only has a complete surface definition through using the multilateral definition of T-spline surface, but also its trimming boundary can be easily altered.

In our future research, we will continue to study the uses of T-spline surface respectively in surface matching, surface lofting, surface sweeping and surface blending, so as to further fulfill the great modeling potential of T-spline surface for car-body surface design.

References:

[1] Liu D C. Research and design of automobile car body CAD system under CADCAM integration environment[J]. Applied Mechanics and Materials, 2014, 443: 44-47.

[2] Prautzsch H, Boehm W, Paluszny M. Bézier and B-spline techniques [M]. Berlin: Springer-Verlag, 2002.

[3] Kuru G, Verhoosel C V, van der Zee K G, et al. Goal-adaptive isogeometric analysis with hierarchical splines[J]. Computer Methods in Applied Mechanics and Engineering, 2014, 270: 270-292.

[4] Bornemann P B, Cirak F. A subdivision-based implementation of the hierarchical B-spline finite element method[J]. Computer Methods in Applied Mechanics and Engineering, 2013, 253: 584-598.

[5] Dokken T, Lyche T, Pettersen K F. Polynomial splines over locally refined box-partitions[J]. Computer Aided Geometric Design, 2013, 30(3): 331-356.

[6] Johannessen K A, Kvamsdal T, Dokken T. Isogeometric analysis using LR B-splines[J]. Computer Methods in Applied Mechanics and Engineering, 2014, 269: 471-514.

[7] Liu W, Zhou X H, Niu Q. 3D geometrical details transfer with cubic B-spline wavelet[J]. Advanced Materials Research, 2014, 889/890:28-31.

[8] Li Y, Ni J. B-spline wavelet-based multiresolution analysis of surface texture in end-milling of aluminum [J]. Journal of Manufacturing Science and Engineering, 2011, 133(1): 011014.

[9] Sederberg T W, Zheng J, Bakenov A, et al. T-splines and T-NURCCs[C]//ACM Transactions on Graphics (TOG). New York, USA: ACM, 2003, 22(3): 477-484.

[10] Sederberg T W, Cardon D L, Finnigan G T, et al. T-spline simplification and local refinement[C]// ACM Transactions on Graphics (TOG). New York, USA: ACM, 2004, 23(3): 276-283.

[11] Tong Weihua, Feng Yuyu, Chen Falai. A surface reconstruction algorithm based on implicit T-spline surfaces[J]. Journal of Computer-Aided Design & Computer Graphics, 2006, 18(3): 358-365. (in Chinese)

[12] Deng J S, Chen F L, Li X, et al. Polynomial splines over hierarchical T-meshes[J]. Graphical Models, 2008, 70(4):76-86.

[13] Kang H M, Chen F L, Deng J S. Modified T-splines [J]. Computer Aided Geometric Design, 2013, 30 (9):827-843.

[14] Carminelli A, Catania G. PB-spline hybrid surface fitting technique[C]//ASME 2009 International Design Engineering Technical Conferences and Computers and Information in Engineering Conference. San Diego, USA: American Society of Mechanical Engineers, 2009: 205-211.

[15] Carminelli A, Catania G. PB-spline finite element shell modeling and refinement technique[C]//ASME 2009 International Design Engineering Technical Conferences and Computers and Information in Engineering Conference. San Diego, USA: American Society of Mechanical Engineers, 2009: 213-221.

(Executive editor: Xu Chengting)